

Article

Sonochemical Reaction of Bifunctional Molecules on Silicon (111) Hydride Surface

Serge Ismael Zida ¹, Yue-Der Lin ^{1,2}  and Yit Lung Khung ^{3,*} 

¹ Ph.D. Program of Electrical and Communications Engineering, College of Information and Electrical Engineering, Feng Chia University, No.100 Wenhwa Road, Seatwen, Taichung 40724, Taiwan; p0766289@o365.fcu.edu.tw (S.I.Z.); ydlin@fcu.edu.tw (Y.D.L.)

² Department of Automatic Control Engineering, Feng Chia University, No.100 Wenhwa Road, Seatwen, Taichung 40724, Taiwan

³ Department of Biological Science and Technology, China Medical University, No.100 Jingmao 1st Road, Beitun District, Taichung City 406, Taiwan

* Correspondence: yitlung.khung@mail.cmu.edu.tw

Abstract: While the sonochemical grafting of molecules on silicon hydride surface to form stable Si–C bond via hydrosilylation has been previously described, the susceptibility towards nucleophilic functional groups during the sonochemical reaction process remains unclear. In this work, a competitive study between a well-established thermal reaction and sonochemical reaction of nucleophilic molecules (cyclopropylamine and 3-Butyn-1-ol) was performed on *p*-type silicon hydride (111) surfaces. The nature of surface grafting from these reactions was examined through contact angle measurements, X-ray photoelectron spectroscopy (XPS) and atomic force microscopy (AFM). Cyclopropylamine, being a sensitive radical clock, did not experience any ring-opening events. This suggested that either the Si–H may not have undergone homolysis as reported previously under sonochemical reaction or that the interaction to the surface hydride via a lone-pair electron coordination bond was reversible during the process. On the other hand, silicon back-bond breakage and subsequent surface roughening were observed for 3-Butyn-1-ol at high-temperature grafting (≈ 150 °C). Interestingly, the sonochemical reaction did not produce appreciable topographical changes to surfaces at the nano scale and the further XPS analysis may suggest Si–C formation. This indicated that while a sonochemical reaction may be indifferent towards nucleophilic groups, the surface was more reactive towards unsaturated carbons. To the best of the author’s knowledge, this is the first attempt at elucidating the underlying reactivity mechanisms of nucleophilic groups and unsaturated carbon bonds during sonochemical reaction of silicon hydride surfaces.

Keywords: sonochemical reaction; sonochemistry; acoustic cavitation; surface grafting; nucleophilic reaction



Citation: Zida, S.I.; Lin, Y.D.; Khung, Y.L. Sonochemical Reaction of Bifunctional Molecules on Silicon (111) Hydride Surface. *Molecules* **2021**, *26*, 6166. <https://doi.org/10.3390/molecules26206166>

Academic Editors: Aneta D. Petelska, Patrycja Dynarowicz-Latka and Klemen Bohinc

Received: 22 August 2021

Accepted: 11 October 2021

Published: 13 October 2021

Publisher’s Note: MDPI stays neutral with regard to jurisdictional claims in published maps and institutional affiliations.



Copyright: © 2021 by the authors. Licensee MDPI, Basel, Switzerland. This article is an open access article distributed under the terms and conditions of the Creative Commons Attribution (CC BY) license (<https://creativecommons.org/licenses/by/4.0/>).

1. Introduction

Silicon is an important industrial element for modern transistors [1,2] as well as being of significant importance to the scientific community in the areas of biotechnology applications [3,4] and in biosensing [5–7]. In surface chemistry, the formation of stable Si–C linkages on silicon surfaces results in highly resilient surfaces that can withstand harsh conditions [8,9]. These surfaces are deemed important in various fields such as in electronics [10–12], semiconductors [13,14], and biosensors [15,16]. Thus far, the literature is rich with various hydrosilylation methodologies ranging from transition metal catalysis [17] to thermal [18,19], ultraviolet initiation [20,21], microwaves activation [22,23] and sonochemical reaction [24], to achieve the formation of stable monolayers on silicon surfaces. Despite being widely reported in literature, these methodologies may have certain limitations. For example, a long reaction time as well as the use of high temperature during thermal reaction increase the chance of unnecessary oxidation [18,25], while both thermal and ultraviolet

strategies can be highly susceptible to surface adventitious carbon contamination [26,27]. Ultraviolet light is also likely to be absorbed and siphoned by aromatic systems when these are the moieties introduced to the silicon surface. Other reaction methods may also have their individual drawbacks. For example, microwave activation, which is very similar to thermal reaction, has a limited depth of penetration into the material [28]. The use of transition metal catalysis could result in difficulty of surface removal of residual catalyst.

Another interesting reaction strategy for grafting monolayer onto a silicon surface is the approach of sonochemical reaction. It can be generally described as the use of ultrasound irradiation to initiate a reaction of a molecule and this process is often performed at a frequency between 15 kHz–10 MHz [29]. During sonochemical reaction on a silicon surface, the dispersive energy of the ultrasound is condensed in the acoustic cavitation which subsequently accelerates the chemical reaction. The basic principle of sonochemical reaction is based on the phenomenon of acoustic cavitation which can be described as the formation, growth and sudden collapse of bubbles induced during sonochemical reaction [29–31]. A significant advantage of sonochemical reaction is that such an approach is inexpensive and environmentally friendly [32]. Other merits also include the simplicity of operation and the uniform dispersion of the ultrasound in the baths [33]. The application of sonochemical reaction is quite broad, ranging from materials synthesis [34,35], nanochemistry [36–38] to simple cleaning [39–41].

In recent years, sonochemical reaction has attracted much interest from surface chemists for the purpose of performing silicon-surface hydrosilylation [24,42]. Notably, Frederick et al., reported the functionalization of organic monolayers of substituted styrenes on silicon hydride surfaces using a range of styrene derivatives [42]. Interestingly, the use of 4-cyanostyrene in their work was of much interest to our group due to the presence of a cyano nucleophilic group that in turn offers an opportunity to examine nucleophiles' competitiveness and preference during the sonochemical process. In fact, their discussion only suggested that the 4-cyanostyrene reaction to the silicon hydride surface under sonochemical reaction occurred through the alkene group instead of the nucleophile but very limited information has been provided for the reasons behind this preference. Hence, at this point of writing, very little is known about the behavior of nucleophiles during a sonochemical-based reaction and a direct comparison between nucleophiles and unsaturated carbon has not yet been reported in literature.

Thus, to shed light into the reaction mechanisms and the preferential bond directionality between unsaturated carbon and nucleophiles during sonochemical reaction, a comparative analysis between sonochemical reaction and thermal excitation was made to conceptualize the overall reaction route of the cyclopropylamine and 3-Butyn-1-ol molecules under both reaction conditions. Thermal reactions of nucleophile were included in this comparative study because our group had previously reported in many accounts the specific preference of nucleophile reacting to silicon hydride surfaces under high temperatures [19,43–45]. This would enable a quick comparison between both reaction processes. The choice of cyclopropylamine was based on its radical susceptibility as described by Nonhebel [46], as this provided us with a window to detect for silicon dangling bonds on the surface which may produce a potential ring opening event of cyclopropylamine. In contrast, 3-Butyn-1-ol has an interesting structure with unsaturated carbon bonds at one end and the hydroxide group at the other end. This structure was important because it gave an opportunity to directly compare the reaction directionality of the molecule (nucleophilic OH or alkyne) during the sonochemical reaction. In the following parts of this work, the surface chemistry analysis through water contact angle measurements, AFM and XPS will be discussed in detail to provide reaction outcomes accordingly.

2. Materials and Methods

In this experiment, P-type silicon (111) (0.001–0.005 Ω cm) was ordered from Semiconductor Wafer, Inc. (Hsinchu, Taiwan). Cyclopropylamine (98%), 3-Butyn-1-ol (97%), Mesitylene (98%), Hydrogen peroxide (30%), Hydrofluoric acid (ACS reagent, 48%) as well

as sulfuric acid (99.99%) were acquired from Sigma-Aldrich (St Louis, MO, USA), except where noted, and used with no further purification.

2.1. Thermal Reaction

P-type silicon (111) wafers were cut in $10 \times 10 \text{ mm}^2$ and cleaned for 30 min in a piranha solution consisting of 1 volume of 33% hydrogen peroxide and 3 volumes of 95% sulfuric acid. Subsequently, a 10% concentration of each compound (Cyclopropylamine and 3-Butyn-1-ol) was diluted in 5 mL mesitylene solution and then transferred to a Schlenk flask for a 15 times freeze–pump–thaw cycle to degas and remove oxygen. After this process, argon gas was added to the Schlenk flask to prevent oxygen from re-entering the solution. The silicon wafers were further cleaned with deionized water and immersed in an aqueous 10% hydrofluoric acid solution for 30 s before being moved to the Schlenk flask solution. The Schlenk flask was submerged in silicon oil for 18 h at 150°C . After the high-temperature thermal reaction, the samples were collected, copiously rinsed and sonicated with methanol, ethanol and deionized water prior to further surface examinations.

2.2. Sonochemical Reaction

P-type silicon wafers (111) were prepared and freeze–pump–thaw cycles were performed in a similar procedure as for the thermal excitation reaction. After transferring the silicon hydride wafers into the solution, the Schlenk flask was then immersed for 2 h at room temperature in the water bath DELTA[®] DC150H sonicator (Delta Ultrasonic Co., Ltd., New Taipei, Taiwan) at a frequency of 40 KHz. Once the reaction was completed, the samples were collected, thoroughly rinsed and sonicated with methanol, ethanol and deionized water before surface analysis. The reaction was identical for each of the compounds, cyclopropylamine and 3-Butyn-1-ol.

2.3. Contact Angle Measurements

The contact angle measurements were performed at China Medical University in Taichung, Taiwan, immediately after the reactions, and the images were obtained via the High View Innovation (HVI) Contact Angle Analyzer (CA1) (Hsinchu, Taiwan). This equipment had a built-in real-time image acquisition and automatic analysis function with an angle measurement from 0 to 180° . A triplicate measurement was performed with a $2 \mu\text{L}$ droplet deposited on the surface of each sample while the automatic measurement deviation was $<1^\circ$. The droplet images were automatically processed and saved using the integrated HVI contact angle software running on a computer with a Windows 10 OS.

2.4. Atomic Force Microscopy Measurements (AFM)

The AFM examinations were conducted at Feng Chia University in Taichung, Taiwan, with the Digital Instrument NS4/D3100CL (Karlsruhe, Germany) MultiMode Scanning Probe Microscope software operating on an integrated AFM tapping mode with cantilever. The frequency of operation was 150 kHz while the Force was 5 N/m. Each of the samples was examined at a scan rate of 0.8 Hz with a scan size of $1 \times 1 \mu\text{m}$. The AFM images were subsequently processed using Gwyddion version 2.59 software running on a Mac OS computer.

2.5. X-ray Photoelectron Spectroscopy (XPS)

The XPS measurements were carried out at National Chung Hsing University (NCHU) in Taichung, Taiwan. An XPS PHI 5000 VersaProbe (ULVAC-PHI) (Kanagawa, Japan) instrument fitted with an Al $K\alpha$ (1486.6 eV) X-ray source was used to perform the analyses. For each of the samples, high-resolution spectra were acquired for C1s, O1s, N1s and Si2p. The deconvolution of the different spectra and the subsequent determination of the full width at half maximum (FWHM) as well as the area under the peak were performed using XPSpeak 4.1 fitting software.

3. Results

Multiple sets of analyses and measurements (triplicates) were conducted after the sample preparation to obtain substantial information to help understand the reactions. Firstly, the outcome of the thermal reactions could be anticipated in view of our previous reports [45,47,48]. More importantly, several questions remained pertaining to how the sonochemical reactions will affect the grafting of the nucleophiles and how the bifunctionality of an alkyne and NH_2 groups may compete with each other during the sonochemical reaction. Contact angle goniometry of the samples was first performed to observe the wettability of the surfaces, as shown in Figure 1a. The contact angle of cyclopropylamine grafting for thermal excitation showed a wetting angle of 85.72° with a deviation margin of $\pm 3.36^\circ$. On the other hand, the water goniometry analysis for the grafting of the same molecule after sonochemical reaction showed an angle of 44.71° with a slight margin of $\pm 2.17^\circ$. The significant difference in contact angle noticed from these observations indicated that the reaction proceeded in a dissimilar fashion for both chemical reactions. The high contact angle for cyclopropylamine thermal reaction was as expected and in trend of agreement with our previous work [47] pertaining to grafting cyclopropylamine with thermal reaction. However, the sessile droplet contact angle registering at 44.71° for the sonochemical reaction sample may be indicative of a different reaction profile that may suggest either polymerization [47,49] or non-reactivity, but at this stage of analysis there was not enough details to make a definitive conclusion.

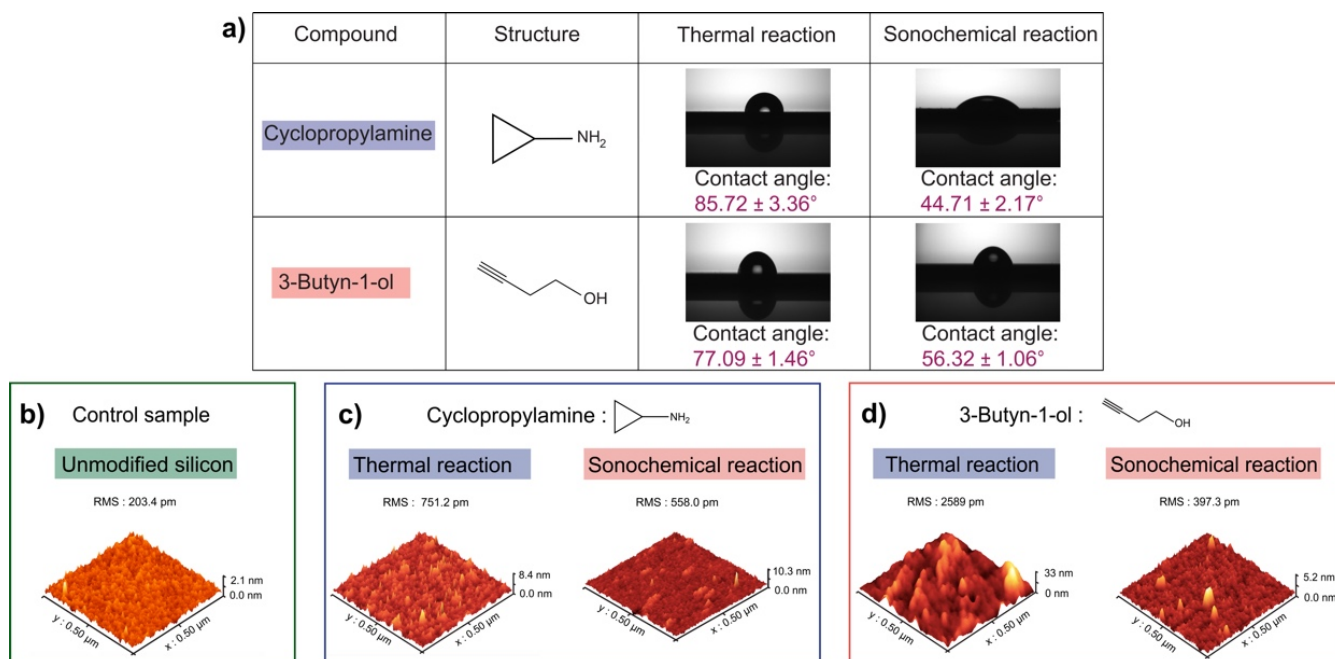


Figure 1. (a) Contact angle measurements of cyclopropylamine and 3-Butyn-1-ol after thermal and sonochemical reaction. (b) AFM examination of the control sample. (c) The AFM characterization of cyclopropylamine showed a roughness value of 751.2 pm for the thermal sample and 558 pm for the sonochemical sample. (d) AFM images of 3-Butyn-1-ol after thermal and sonochemical reaction.

For 3-Butyn-1-ol molecule, the first set of measurements was performed on the thermal reaction sample and the triple sampling had presented a wettability profile of $77.09^\circ \pm 1.46^\circ$. However, for the sonochemical reaction sample, a lower angle of $56.32^\circ \pm 1.06^\circ$ was noted. As usual, although there was a difference in the wettability profile between sonochemical and thermal reaction, it was not substantial enough to make an assumption at this point. Therefore, additional surface analyses were necessary to understand the possible reaction outcomes and AFM examinations were performed to observe the surface topography as well as to determine the surface roughness for each of the samples.

The AFM examination of the control sample displayed a surface with very little roughness, and the RMS value was approximately 203.4 pm as shown in Figure 1b. Compared with the control sample, some changes were observed on the surface topography of the cyclopropylamine-based thermal reaction with a RMS value of 751.2 pm which, in conjunction with the high contact angle and our past works [19,47], could indicate that a reaction occurred via the nucleophilic group. For the cyclopropylamine sonochemical reaction sample, the previous observation of the low contact angle may have suggested polymerization of the surface. If polymerization did occur, the AFM study should show a thickening layer on the surface. However, such a result was not observed in the AFM examination (as shown in Figure 1c). The RMS value of the sample was 558 pm, and it was interesting to note that this value had tilted towards that of the control sample, but the slight roughening may be explained by the fact that the control sample was not influenced by the etching effect of hydrofluoric acid during the sample preparation.

In Figure 1d, the surface examinations of the sample of 3-Butyn-1-ol after thermal reaction showed a characterized surface roughness, and the RMS value was 2589 pm. In contrast, for the sample of 3-Butyn-1-ol after sonochemical reaction, the RMS decreased significantly to 397.3 pm while significant topographical changes were exhibited on the surface. This low RMS value may be due to the fact that the reaction did not take place or did occur through the formation of a Si–C bond, and the OH group was presented as a distal group, which could also explain the lower contact observed for the sample. Nevertheless, XPS experiments were needed to make further deductions or to support some early hypothesis.

XPS studies were carried out to provide more information on the nature of the bond formation mechanism, especially in the presence of nucleophilic groups. As shown in Figure 2a, the analysis of the Si2p spectrum of the control sample indicated 3 peaks at 99.1 eV, 99.8 eV and 102.7, which was, respectively, representative of Si2p_{3/2}, Si2p_{1/2} and Si–O_x as described previously [50,51]. Furthermore, the Si2p spectrum of the thermal reaction of cyclopropylamine displayed the Si2p_{3/2} and Si2p_{1/2} peaks at 98.7 and 99.3 eV, respectively (as demonstrated in Figure 2b). A peak was fitted at 101.9 eV, which was +3.2 eV shift from the Si2p_{3/2} peak and was typical of Si–N bonding as described by Luo et al. [52] as well as by our previous studies [19,47,48]. The presence of the Si–N bond was indicative that thermal reaction had occurred through the amine group and this was in corroboration with previous accounts [47]. The Si–O_x peak was fitted at 103 eV and was a shift of +4.3 eV from the Si2p_{3/2} peak [53,54].

On the other hand, in silicon surfaces that underwent a cyclopropylamine-based sonochemical reaction, the analysis of the spectra did not detect the presence of Si–N linkage. The Si2p_{3/2} and Si2p_{1/2} peaks were observed at 99.1 and 99.8 eV, while a peak at 102.6 eV was attributed to Si–O_x as described by Yoon et al. [55]. In comparison with the control sample, it can be noticed that both samples have similar peaks at approximately the same binding energy position, and this further confirmed that the surface grafting may not have occurred for a cyclopropylamine-based sonochemical reaction.

The XPS deconvolution of the 3-Butyn-1-ol sample for thermal excitation showed a single peak at 101.4 eV that was characteristic of Si–O–X [45]. The presence of a single peak can be explained by the concentration level of 3-Butyn-1-ol (10% concentration in this study). As demonstrated in the past [45], as the concentration of 3-Butyn-1-ol increased, the spectrum tended to lose its Si2p peaks and the reaction proceeded through the nucleophile OH to form Si–O–C bonds at the surface. On the contrary, for the sonochemical reaction, three distinct peaks were successfully fitted during the deconvolution. The Si2p_{3/2}, Si2p_{1/2} and Si–O_x peaks were observed at 99, 99.7 and 102.6 eV, respectively [55], as shown in Figure 2e. Lower oxidation was detected as compared with the control surface and our attempt to fit a Si–C peak at around 101.2–101.6 eV was not successful. Hence, additional deconvolution of the C1s spectra was therefore necessary.

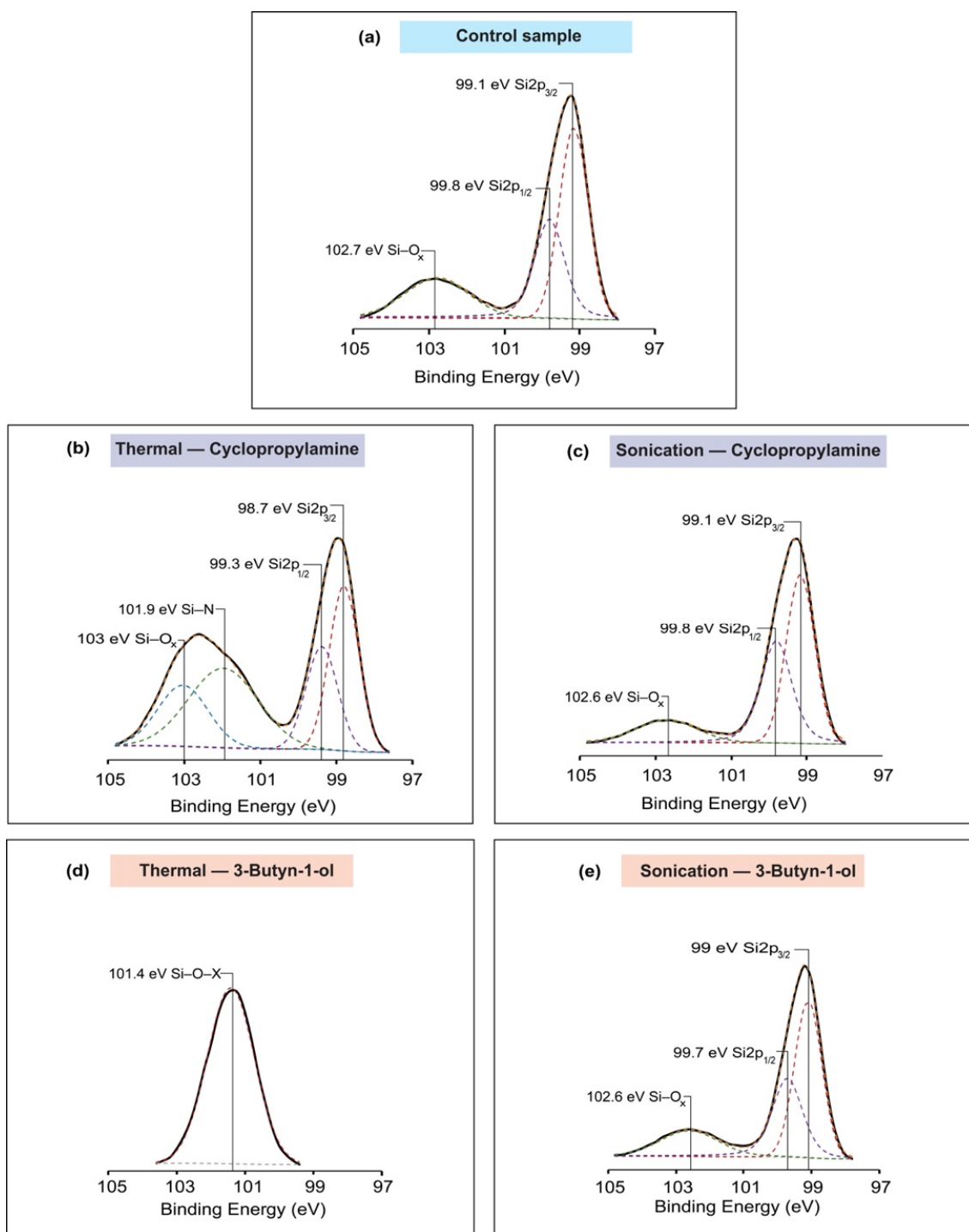


Figure 2. Si₂p spectrum deconvolution for (a) control sample; (b) cyclopropylamine thermal excitation. A silicon nitrogen peak appeared at 101.9 eV; (c) cyclopropylamine sonochemical reaction; (d) 3-Butyn-1-ol thermal excitation with a single peak fitted at 101.4 eV; (e) 3-Butyn-1-ol sonochemical reaction.

The spectrum of the high-resolution C₁s spectra of the samples had shown the C–C peaks at 284.4–284.8 eV [56–58] and C–O peaks at 286.2–286.3 eV [59,60]. For cyclopropylamine-based thermal reaction, a peak was observed at 286 and 287.7 eV which were, respectively, indicative of a C–N bond [61,62] and O=C–N bond [63–65] as presented in Figure 3b. However, for the sonochemical reaction of cyclopropylamine, the absence of C–N bond was another reinforcing proof that the reaction did not take place through the nucleophile NH₂. On the other hand, by comparing the C₁s analysis of 3-Butyn-1-ol thermal to the sonochemical reaction, a peak at

the 287.2 eV position (Figure 3e) was successfully fitted for the sonochemical reaction sample and was characteristic of a C=O bond [66,67]. More importantly, as highlighted in Figure 3e, a notch was noticed at about 282.2 eV and this could be representative of Si-C bonding, as described by Wang et al. [68].

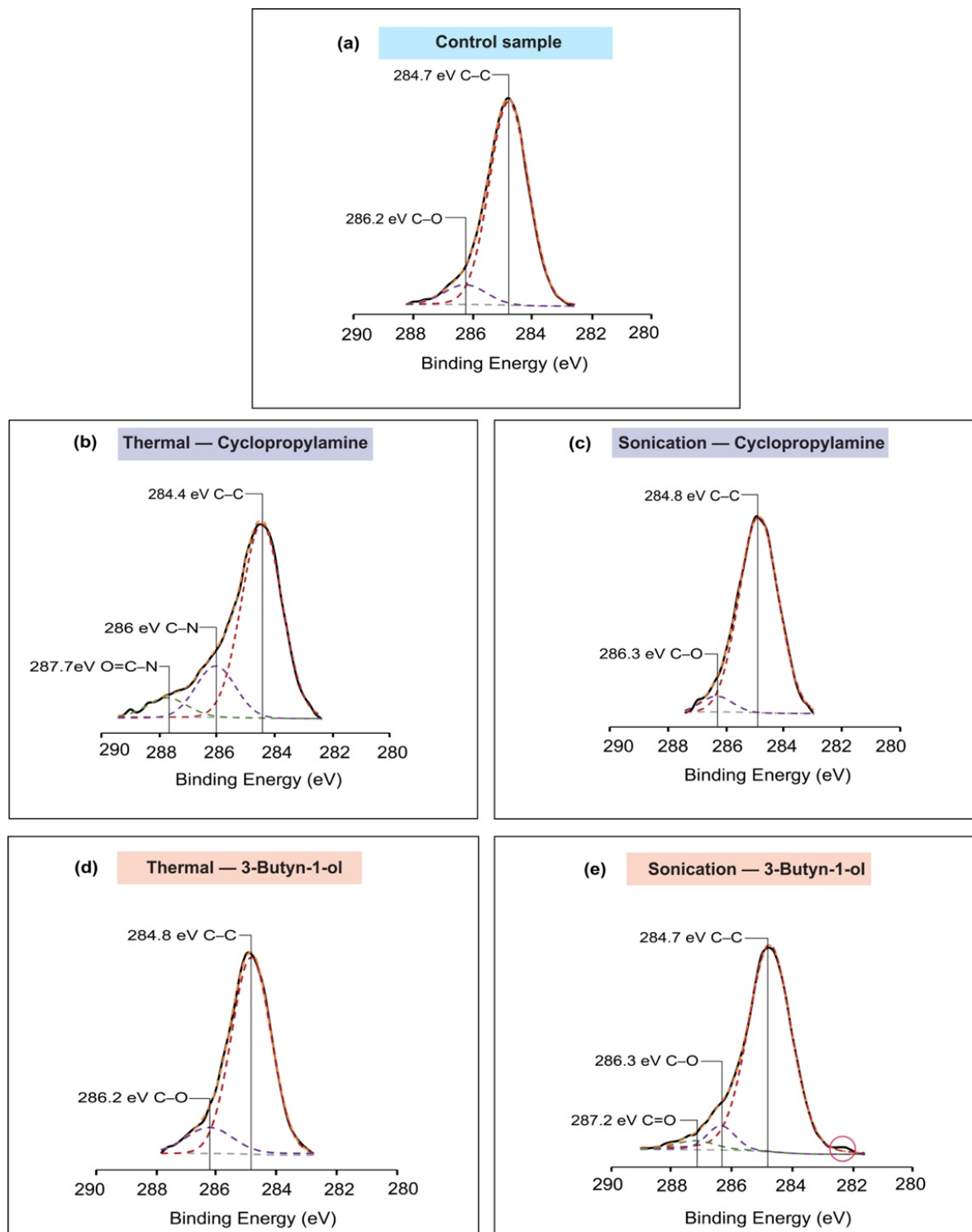


Figure 3. The analysis of the C1s spectra of each sample. (a) Control sample; (b) cyclopropylamine thermal reaction with C-N and O=C-N linkage type; (c) cyclopropylamine sonochemical reaction; (d) 3-Butyn-1-ol thermal excitation; (e) 3-Butyn-1-ol sonochemical reaction with carbon-carbon and carbon-oxygen peaks. The outlined part suggested that the reaction may have occurred.

The deconvolution of the O1s spectrum was necessary to identify the nature of the oxygen bonds. A single peak was fitted at a position of 532.4 eV for the control sample, which was representative of Si–O bonding [69]. Furthermore, two peaks were successfully fitted in the thermal reaction spectrum analysis of 3-Butyn-1-ol. As shown in Figure 4b, the smaller peak at the same position of 532.4 eV indicated a Si–O/C–O linkage type while the larger peak fitted at 531.1 eV was representative of Si–O–C bond [45,70]. Comparatively, the deconvolution of the sonochemical reaction sample resulted in a unique peak at 532.2 eV which was suggestive of a Si–O/C–O bonding type [71,72]. These findings further support that the sonochemical-based reaction did not occur through the OH group with the formation of Si–O–C bonds, but rather might have taken place via the alkyne group with the formation of a Si–C bond. The different peaks from the O1s spectra analysis were as displayed in Figure 4.

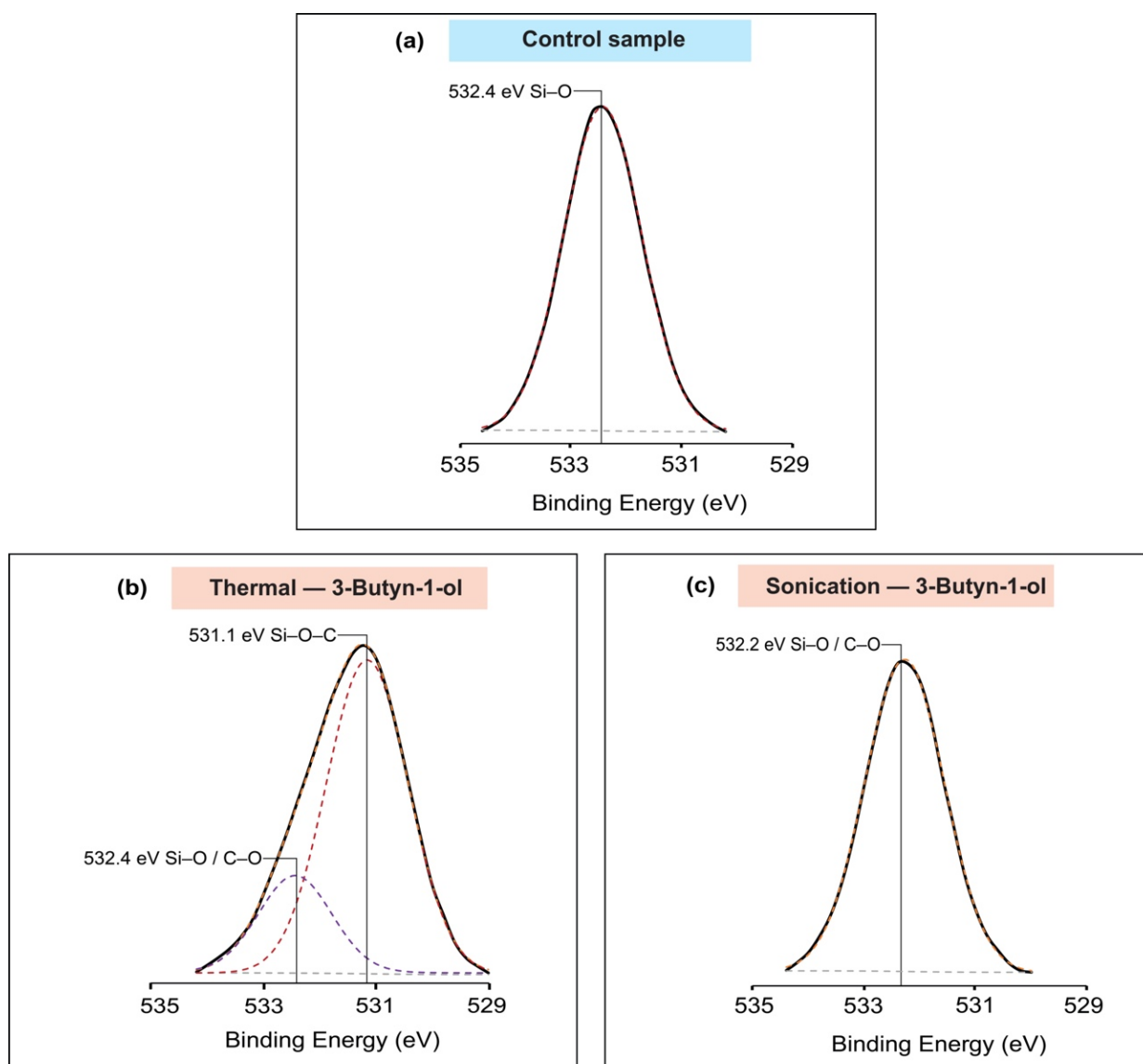


Figure 4. Deconvolution of the high-resolution O1s spectra (a) control sample; (b) thermal reaction of 3-Butyn-1-ol with two peaks observed at 531.1 and 532.4 eV; (c) sonochemical reaction of 3-Butyn-1-ol.

The high-resolution N1s spectra studies were also important to comprehend the details of nitrogen bond formation. To better correlate the relative nitrogen levels among the samples, the intensity of the spectrum was kept consistent for each of the samples. As shown in Figure 5a, a relatively flat spectrum was observed for the control sample, which

was expected since the surface did not undergo any modifications. More interestingly, when comparing the thermal reaction of cyclopropylamine (Figure 5b) to the sonochemical reaction (Figure 5c), a significant peak was noticed at about 399 eV for the thermal reaction while the sonochemical reaction sample showed a plain spectrum without relevant peaks. Based on the literature [73,74], the peak positioned at about 399 eV was found to correspond to the formation of Si–N bonds, thus further confirming that the reaction had occurred through the nucleophile NH₂. On the other hand, the observation of the flat spectrum for the sonochemical reaction provided further evidence that the sonochemical reaction did not induce any chemical reaction of cyclopropylamine.

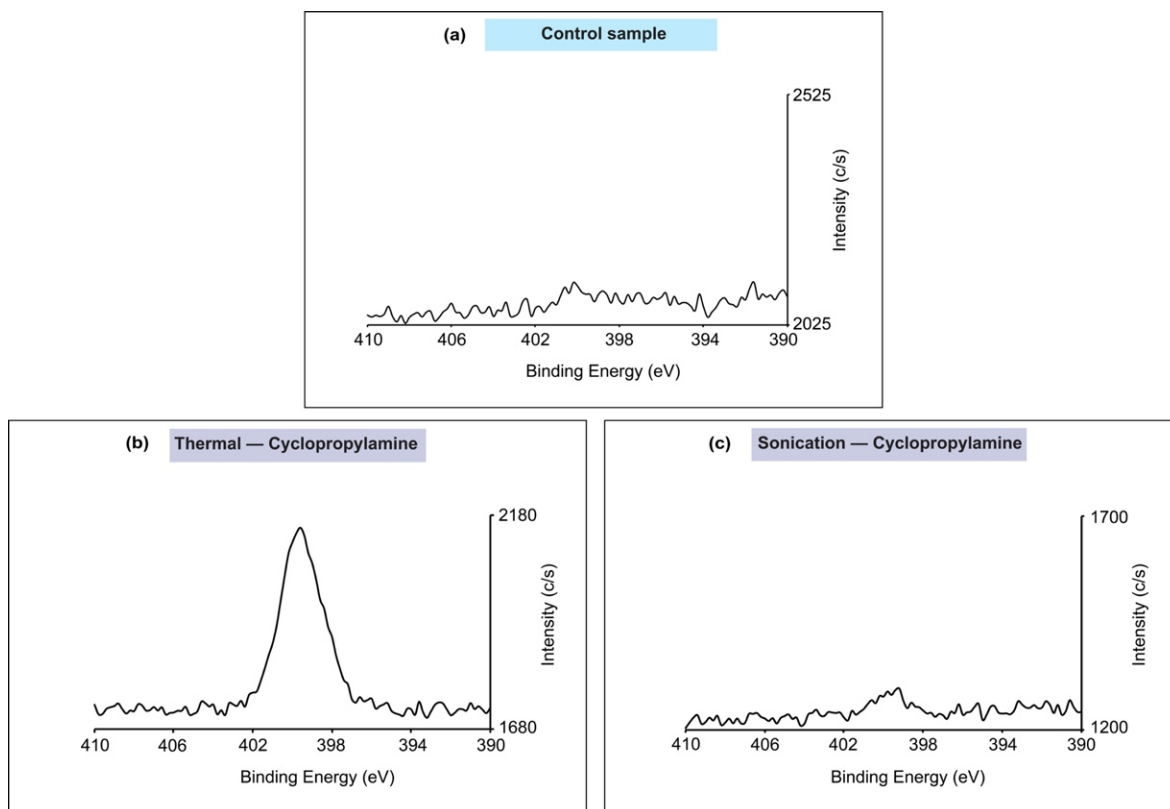


Figure 5. N1s spectra analysis for (a) control sample; (b) cyclopropylamine thermal reaction; (c) cyclopropylamine sonochemical reaction. Both samples (a,c) showed relatively flat spectrum while the thermal reaction of cyclopropylamine produced a significant peak at around 399 eV.

The assignments discussed in this study, along with their corresponding binding energy, FWHM and area under the peak, have been summarized in Table 1. The different peaks described in this table were in good agreement with the formation of corresponding chemical bonds as documented in the literature. The combined analysis of this information was substantial in our effort to understand the different types of chemical bonding.

Table 1. Representative summary of peak assignments reported in this work.

Reaction Model	Binding Energy (eV)	Assignment	FWHM	Area under the Peak
Control Sample	99.1	Si2p _{3/2}	0.9	6997.69
	99.8	Si2p _{1/2}	0.93	4361.18
	102.7	Si–O _x	2.02	3225.73
	284.7	C–C	1.53	4289.18
	286.2	C–O	1.65	458.30
	532.4	Si–O	1.67	17,751.58

Table 1. Cont.

Reaction Model		Binding Energy (eV)	Assignment	FWHM	Area under the Peak	
Cyclopropylamine	Thermal reaction	98.7	Si2p _{3/2}	0.91	2767.26	
		99.3	Si2p _{1/2}	0.98	1855.55	
		101.9	Si–N	2.17	3135.52	
		103	Si–O _x	1.55	1730.05	
	C1s	284.4	C–C	1.64	3814.62	
		286	C–N	1.62	1000.39	
		287.7	O=C–N	1.66	439.55	
	Sonochemical reaction	Si2p	99.1	Si2p _{3/2}	0.88	6271.15
			99.8	Si2p _{1/2}	0.95	4823.99
			102.6	Si–O _x	1.89	1720.59
		C1s	284.8	C–C	1.57	2897.68
			286.3	C–O	1.27	185.57
	3-Butyn-1-ol	Thermal reaction	101.4	Si–O–X	1.64	3279.78
			284.8	C–C	1.54	3182.46
286.2			C–O	1.78	469.47	
531.1			Si–O–C	1.72	10,290.74	
Sonochemical reaction		Si2p	99	Si2p _{3/2}	0.95	5912.40
			99.7	Si2p _{1/2}	1.05	3856.94
		C1s	102.6	Si–O _x	1.96	1979.99
			284.7	C–C	1.68	4057.23
O1s	286.3	C–O	1.07	280.74		
	287.2	C=O	1.46	140.44		
532.2	Si–O/C–O	1.68	10,898.10			

4. Discussion

The data acquired through the contact angle measurements in conjunction with the AFM studies and XPS analysis were necessary in our attempt to describe how the directionality of the reaction had occurred. However, prior to discussing the outcome of the reactions in this work, it was important to describe the basic mechanisms that might have taken place during the sonochemical reaction. The underlying mechanism of sonochemical reaction has been discussed in literature in the past by various groups providing contradictory arguments, and this consequently demonstrated the complexity in attempts to elucidate the precise mechanism during sonochemical reactions. Ando et al., were the first to suggest that sonochemical reaction may affect nucleophilic substitutions outcomes [75]. They reported that during sonochemical reaction, waves from ultrasound may accelerate the nucleophilic attack of the alumina surface by the leaving group, hence resulting in a nucleophilic substitution event. This initial study was the first to propose a reaction mechanism that could occur during the sonochemical activation process. Luche et al., subsequently attempted to digress sonochemical reaction in different environments by discussing the concept of ‘true’ and ‘false’ sonochemical reaction [76]. In their context, ‘true’ sonochemical reaction was described as a reaction in which acoustic cavitation creates a coordinated unsaturated element and free radicals to influence the chemical outcome of the reaction in homogeneous solution, while the outcome of the ‘false’ sonochemical reaction was due to the mechanistic impact of sonochemical reaction in a heterogeneous solution. The notion that a sonochemical-based reaction is merely a mechanistic rather than a chemical

operation was also discussed by Kegelaers et al. [77] who, after repeating the same series of experiments as described by Ando et al. [75], came to the different conclusion that sonochemical reaction served as a mechanistic approach akin to those from extensive stirring that shortens the reaction time [78] but by itself did not induce a chemical change. Despite various examples of ‘true’ [79–81] and ‘false’ [82,83] sonochemical reactions in literature, which so far remain as the most common explanations, it is necessary to acknowledge that the exact mechanism of sonication chemistry has not yet been clearly elucidated [84].

Prior to this work, we had demonstrated that during a thermal excitation reaction, cyclopropylamine reaction to silicon hydride surface occurred via the NH_2 nucleophilic group to form Si–N bonds [47] while 3-Butyn-1-ol reacts to silicon hydride through the OH group to form a Si–O–C bond [45]. These preferences were largely due to the fact that the electronegative domain from the nucleophile tends to offer precedence over unsaturated carbon groups. The main question to address in this study was to determine the reaction directionality of these bifunctional molecules during the sonochemical process. In the cyclopropylamine-based sonochemical reaction, the absence of Si–N bonds observed in the Si2p spectrum (Figure 2c), along with the lack of surface reorganization due to oxidation as shown in the AFM studies (Figure 1b), could indicate that the nucleophilic group did not react aggressively to the silicon hydride surface. This non-reaction of the nucleophile on the silicon hydride surface can be explained by the effect of acoustic cavitation, whose violent collapse could continue to break the coordinative bonds upon surface formation. In fact, the mechanical effect of sonochemical reaction has shown to induce coordination bond breaking, as reported by Paulusse et al. [85]. The continuous cycle of bond formation and breakage could explain the non-reaction observed during sonochemical reaction. Moreover, during sonochemical reaction, despite the fact that the explosion of bubbles due to acoustic cavitation produces a high temperature, such a high temperature lasts only a few microseconds, as described by Suslick [29], and may not be sustainable enough to initiate a chemical reaction of the nucleophilic group. The absence of sustained heat generated during the sonochemical reaction might also lead the silicon hydride surface to repel the cyclopropane nucleophilic group from the surface.

On the other hand, for the 3-Butyn-1-ol-based sonochemical reaction, the silicon hydride surface reacted to the unsaturated carbon of the molecule to form Si–C bonds and this was as observed in Figure 3e. The mechanism of this reaction with the silicon surface still remains complex; however, some elements of responses can be found in the work reported by Korgel’s group [86]. They described that during hydrosilylation reaction at room temperature, there is a mechanism where the nucleophilic group correlates to the silicon surface to increase the reactivity of the hydrogenated silicon surface, thus leading to the extension of the Si–H bond. The extended Si–H bond can then react with other unsaturated carbons of the same molecule. From these analyses, the final reaction pathway of both cyclopropylamine and 3-Butyn-1-ol can be described as illustrated in Figure 6.

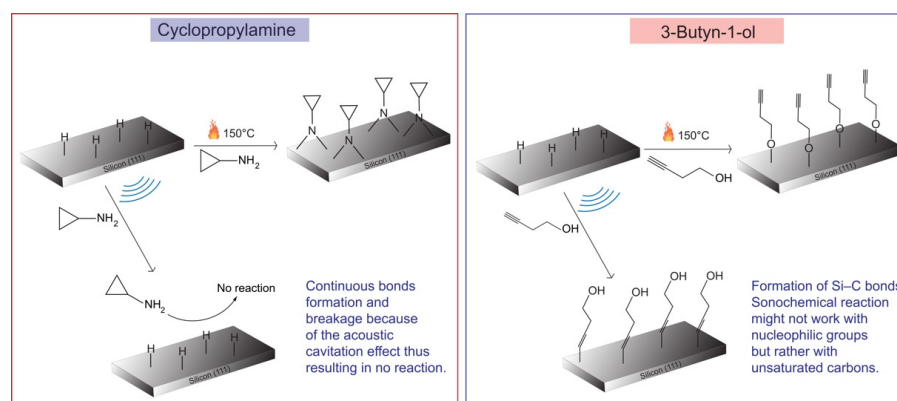


Figure 6. Proposed schematic of the reaction pathways for the grafting of cyclopropylamine and 3-Butyn-1-ol during high-temperature thermal and sonochemical reaction.

5. Conclusions

Sonochemical reaction is an interesting activation method for surface characterization because it offers a good reaction rate [87] as well as the possibility to understand the influence of ultrasound on chemical bond formation on planar silicon surfaces. In this report, we carefully examined the reaction preferences of nucleophiles and unsaturated carbon in bifunctional molecules, and we subsequently proposed a reaction pathway for the grafting of the molecules based on the analysis of the experimental results of both reactions. The results from thermal reaction serving as our guide had suggested direct nucleophilic addition to the silicon hydride surface, thus resulting in the formation of silicon nitride bonds on the surface, while the sonochemical activation with the effect of acoustic cavitation does not induce a similar reaction profile due to the hypothesized process of constant dative bond formation and breakage as a result of acoustic cavitation on the surface. In contrast, with the 3-Butyn-1-ol which has an alkyne and a nucleophile end, the sonochemical reaction preferentially takes place through the alkyne group of the molecule that in turn stabilizes the surface grafting even during the process of acoustic cavitation. Furthermore, observations from our thermal reaction also support the claim that the reaction inversely occurs through the hydroxide group. These findings are important as they provide more insights into the underlying mechanism of sonochemical reaction and could further open up an avenue of research to understand the behavior of nucleophile and alkyne during this process.

Author Contributions: S.I.Z. performed the experiments of sample preparation, the data curation and analysis, as well as writing the manuscript. Y.D.L. supervised, financed and reviewed the content of this manuscript. Y.L.K. conceptualized, funded the project, supervised and reviewed the manuscript. All authors have read and agreed to the published version of the manuscript.

Funding: This work was financially supported by grants from the Ministry of Science and Technology, Taiwan (MOST 109-2221-E-039-013-MY2 and MOST 110-2221-E-035-006-MY3) and from China Medical University (CMU109-S-02).

Institutional Review Board Statement: Not applicable.

Informed Consent Statement: Not applicable.

Data Availability Statement: Not applicable.

Conflicts of Interest: The authors declare no conflict of interest.

Sample Availability: Samples of the compounds cyclopropylamine and 3-Butyn-1-ol are available from the authors.

References

1. Lang, W. Silicon microstructuring technology. *Mater. Sci. Eng. R. Rep.* **1996**, *17*, 1–55. [[CrossRef](#)]
2. Jeong, M.; Doris, B.; Kedzierski, J.; Rim, K.; Yang, M. Silicon Device Scaling to the Sub-10-nm Regime. *Science* **2004**, *306*, 2057–2060. [[CrossRef](#)] [[PubMed](#)]
3. Bond, R.; McAuliffe, J.C. Silicon biotechnology: New opportunities for carbohydrate science. *Aust. J. Chem.* **2003**, *56*, 7–11. [[CrossRef](#)]
4. Morse, D.E. Silicon biotechnology: Harnessing biological silica production to construct new materials. *TRENDS Biotechnol.* **1999**, *17*, 230–232. [[CrossRef](#)]
5. Zida, S.I.; Yang, C.-C.; Khung, Y.L.; Lin, Y.-D. Fabrication and Characterization of an Aptamer-Based N-type Silicon Nanowire FET Biosensor for VEGF Detection. *J. Med. Biol. Eng.* **2020**, *40*, 601–609. [[CrossRef](#)]
6. Chhasatia, R.; Sweetman, M.J.; Prieto-Simon, B.; Voelcker, N.H. Performance optimisation of porous silicon rugate filter biosensor for the detection of insulin. *Sens. Actuators B Chem.* **2018**, *273*, 1313–1322. [[CrossRef](#)]
7. Tran, D.P.; Pham, T.T.T.; Wolfrum, B.; Offenhäusser, A.; Thierry, B. CMOS-compatible silicon nanowire field-effect transistor biosensor: Technology development toward commercialization. *Materials* **2018**, *11*, 785. [[CrossRef](#)] [[PubMed](#)]
8. Sieval, A.B.; Demirel, A.L.; Nissink, J.W.M.; Linford, M.R.; van der Maas, J.H.; de Jeu, W.H.; Zuilhof, H.; Sudhölter, E.J.R. Highly Stable Si–C Linked Functionalized Monolayers on the Silicon (100) Surface. *Langmuir* **1998**, *14*, 1759–1768. [[CrossRef](#)]
9. Terry, J.; Linford, M.R.; Wigren, C.; Cao, R.; Pianetta, P.; Chidsey, C.E.D. Determination of the bonding of alkyl monolayers to the Si(111) surface using chemical-shift, scanned-energy photoelectron diffraction. *Appl. Phys. Lett.* **1997**, *71*, 1056–1058. [[CrossRef](#)]

10. Vilan, A.; Yaffe, O.; Biller, A.; Salomon, A.; Kahn, A.; Cahen, D. Molecules on Si: Electronics with Chemistry. *Adv. Mater.* **2010**, *22*, 140–159. [[CrossRef](#)]
11. Cerofolini, G.; Mascolo, D. A hybrid micro-nano-molecular route for nonvolatile memories. *Semicond. Sci. Technol.* **2006**, *21*, 1315. [[CrossRef](#)]
12. Aswal, D.K.; Lenfant, S.; Guerin, D.; Yakhmi, J.V.; Vuillaume, D. Self assembled monolayers on silicon for molecular electronics. *Anal. Chim. Acta* **2006**, *568*, 84–108. [[CrossRef](#)]
13. Roth, K.M.; Yasserli, A.A.; Liu, Z.; Dabke, R.B.; Malinovskii, V.; Schweikart, K.-H.; Yu, L.; Tiznado, H.; Zaera, F.; Lindsey, J.S.; et al. Measurements of Electron-Transfer Rates of Charge-Storage Molecular Monolayers on Si(100). Toward Hybrid Molecular/Semiconductor Information Storage Devices. *J. Am. Chem. Soc.* **2003**, *125*, 505–517. [[CrossRef](#)] [[PubMed](#)]
14. Bent, S.F. Organic functionalization of group IV semiconductor surfaces: Principles, examples, applications, and prospects. *Surf. Sci.* **2002**, *500*, 879–903. [[CrossRef](#)]
15. Touahir, L.; Allongue, P.; Aureau, D.; Boukherroub, R.; Chazalviel, J.N.; Galopin, E.; Gouget-Laemmel, A.C.; de Villeneuve, C.H.; Moraillon, A.; Niedziółka-Jönsson, J.; et al. Molecular monolayers on silicon as substrates for biosensors. *Bioelectrochemistry* **2010**, *80*, 17–25. [[CrossRef](#)] [[PubMed](#)]
16. Masood, M.N.; Chen, S.; Carlen, E.T.; Berg, A.v.d. All-(111) Surface Silicon Nanowires: Selective Functionalization for Biosensing Applications. *ACS Appl. Mater. Interfaces* **2010**, *2*, 3422–3428. [[CrossRef](#)] [[PubMed](#)]
17. Zazzera, L.A.; Evans, J.F.; Deruelle, M.; Tirrell, M.; Kessel, C.R.; McKeown, P. Bonding Organic Molecules to Hydrogen-Terminated Silicon Wafers. *J. Electrochem. Soc.* **1997**, *144*, 2184–2189. [[CrossRef](#)]
18. Boukherroub, R.; Wojtyk, J.T.C.; Wayner, D.D.M.; Lockwood, D.J. Thermal Hydrosilylation of Undecylenic Acid with Porous Silicon. *J. Electrochem. Soc.* **2002**, *149*, H59. [[CrossRef](#)]
19. Tung, J.; Tew, L.S.; Coluccini, C.; Lin, Y.-D.; Khung, Y.L. Grafting Behavior for the Resonating Variants of Ethynylaniline on Hydrogenated Silicon (100) Surfaces under Thermal Hydrosilylation. *Chemistry* **2018**, *24*, 13270–13277. [[CrossRef](#)]
20. Huck, L.A.; Buriak, J.M. UV-Initiated Hydrosilylation on Hydrogen-Terminated Silicon (111): Rate Coefficient Increase of Two Orders of Magnitude in the Presence of Aromatic Electron Acceptors. *Langmuir* **2012**, *28*, 16285–16293. [[CrossRef](#)]
21. Terry, J.; Mo, R.; Wigren, C.; Cao, R.; Mount, G.; Pianetta, P.; Linford, M.R.; Chidsey, C.E. Reactivity of the H-Si (111) surface. *Nucl. Instrum. Methods Phys. Res. Sect. B Beam Interact. Mater. At.* **1997**, *133*, 94–101. [[CrossRef](#)]
22. Boukherroub, R.; Petit, A.; Loupy, A.; Chazalviel, J.-N.; Ozanam, F. Microwave-Assisted Chemical Functionalization of Hydrogen-Terminated Porous Silicon Surfaces. *J. Phys. Chem. B* **2003**, *107*, 13459–13462. [[CrossRef](#)]
23. Small, J.C.; Dam, H.M.; Siegel, J.L.; Crepinsek, A.J.; Neal, T.A.; Althoff, A.A.; Line, N.S.; Porter, L.A. Alkyl-functionalization of porous silicon via multimode microwave-assisted hydrosilylation. *Polyhedron* **2016**, *114*, 225–231. [[CrossRef](#)]
24. Zhong, Y.L.; Bernasek, S.L. Mild and Efficient Functionalization of Hydrogen-Terminated Si(111) via Sonochemical Activated Hydrosilylation. *J. Am. Chem. Soc.* **2011**, *133*, 8118–8121. [[CrossRef](#)]
25. Boukherroub, R.; Wayner, D.D.M.; Sproule, G.I.; Lockwood, D.J.; Canham, L.T. Stability Enhancement of Partially-Oxidized Porous Silicon Nanostructures Modified with Ethyl Undecylenate. *Nano Lett.* **2001**, *1*, 713–717. [[CrossRef](#)]
26. Ciampi, S.; Harper, J.B.; Gooding, J.J. Wet chemical routes to the assembly of organic monolayers on silicon surfaces via the formation of Si–C bonds: Surface preparation, passivation and functionalization. *Chem. Soc. Rev.* **2010**, *39*, 2158–2183. [[CrossRef](#)]
27. Cerofolini, G.F.; Galati, C.; Reina, S.; Renna, L. Functionalization of the (100) surface of hydrogen-terminated silicon via hydrosilylation of 1-alkyne. *Mater. Sci. Eng. C* **2003**, *23*, 253–257. [[CrossRef](#)]
28. De La Hoz, A.; Alcázar, J.; Carrillo, J.; Herrero, M.A.; Muñoz, J.D.M.; Prieto, P.; De Cózar, A.; Diaz-Ortiz, A. *Reproducibility and Scalability of Microwave-Assisted Reactions*; IntechOpen: London, UK, 2011.
29. Suslick, K.S. Sonochemistry. *Science* **1990**, *247*, 1439–1445. [[CrossRef](#)]
30. Leighton, T.G. Bubble population phenomena in acoustic cavitation. *Ultrason. Sonochem.* **1995**, *2*, S123–S136. [[CrossRef](#)]
31. Theerthagiri, J.; Madhavan, J.; Lee, S.J.; Choi, M.Y.; Ashokkumar, M.; Pollet, B.G. Sonochemistry for energy and environmental applications. *Ultrason. Sonochem.* **2020**, *63*, 104960. [[CrossRef](#)]
32. Chatel, G.; Varma, R.S. Ultrasound and microwave irradiation: Contributions of alternative physicochemical activation methods to Green Chemistry. *Green Chem.* **2019**, *21*, 6043–6050. [[CrossRef](#)]
33. Mason, T.J.; Peters, D. *Practical Sonochemistry: Power Ultrasound Uses and Applications*; Elsevier Science: Amsterdam, The Netherlands, 2002.
34. Colmenares, J.C. Sonication-induced pathways in the synthesis of light-active catalysts for photocatalytic oxidation of organic contaminants. *ChemSusChem* **2014**, *7*, 1512–1527. [[CrossRef](#)] [[PubMed](#)]
35. Pinjari, D.; Prasad, K.; Gogate, P.; Mhaske, S.; Pandit, A. Synthesis of titanium dioxide by ultrasound assisted sol-gel technique: Effect of calcination and sonication time. *Ultrason. Sonochem.* **2015**, *23*, 185–191. [[CrossRef](#)] [[PubMed](#)]
36. Gedanken, A. Sonochemistry and its application to nanochemistry. *Curr. Sci.* **2003**, *85*, 1720–1722.
37. Afreen, S.; Muthoosamy, K.; Manickam, S. Sono-nano chemistry: A new era of synthesising polyhydroxylated carbon nanomaterials with hydroxyl groups and their industrial aspects. *Ultrason. Sonochem.* **2019**, *51*, 451–461. [[CrossRef](#)] [[PubMed](#)]
38. Yu, Y.; Theerthagiri, J.; Lee, S.J.; Muthusamy, G.; Ashokkumar, M.; Choi, M.Y. Integrated technique of pulsed laser irradiation and sonochemical processes for the production of highly surface-active NiPd spheres. *Chem. Eng. J.* **2021**, *411*, 128486. [[CrossRef](#)]
39. Tuziuti, T. Influence of sonication conditions on the efficiency of ultrasonic cleaning with flowing micrometer-sized air bubbles. *Ultrason. Sonochem.* **2016**, *29*, 604–611. [[CrossRef](#)] [[PubMed](#)]

40. Farmer, A.; Collings, A.; Jameson, G. Effect of ultrasound on surface cleaning of silica particles. *Int. J. Mineral. Process.* **2000**, *60*, 101–113. [[CrossRef](#)]
41. Theerthagiri, J.; Lee, S.J.; Karuppasamy, K.; Arulmani, S.; Veeralakshmi, S.; Ashokkumar, M.; Choi, M.Y. Application of advanced materials in sonophotocatalytic processes for the remediation of environmental pollutants. *J. Hazard. Mater.* **2021**, *412*, 125245. [[CrossRef](#)]
42. Frederick, E.; Dickerson, P.N.; Zhong, Y.L.; Bernasek, S.L. Substituent Effects on the Kinetics of Bifunctional Styrene SAM Formation on H-Terminated Si. *Langmuir* **2014**, *30*, 7687–7694. [[CrossRef](#)]
43. Khung, Y.L.; Ngalm, S.H.; Scaccabarozi, A.; Narducci, D. Thermal and UV Hydrosilylation of Alcohol-Based Bifunctional Alkynes on Si (111) surfaces: How surface radicals influence surface bond formation. *Sci. Rep.* **2015**, *5*, 11299. [[CrossRef](#)]
44. Khung, Y.L.; Ngalm, S.H.; Meda, L.; Narducci, D. Preferential Formation of Si–O–C over Si–C Linkage upon Thermal Grafting on Hydrogen-Terminated Silicon (111). *Chemistry* **2014**, *20*, 15151–15158. [[CrossRef](#)]
45. Lee, C.H.; Khung, Y.L. Molecular geometry influencing thermal-based nucleophilic reactions on silicon (111) hydride surfaces. *Appl. Surf. Sci.* **2020**, *527*, 146697. [[CrossRef](#)]
46. Nonhebel, D.C. The chemistry of cyclopropylmethyl and related radicals. *Chem. Soc. Rev.* **1993**, *22*, 347–359. [[CrossRef](#)]
47. Tung, J.; Ching, J.Y.; Ng, Y.M.; Tew, L.S.; Khung, Y.L. Grafting of Ring-Opened Cyclopropylamine Thin Films on Silicon (100) Hydride via UV Photoionization. *ACS Appl. Mater. Interfaces* **2017**, *9*, 31083–31094. [[CrossRef](#)] [[PubMed](#)]
48. Ching, J.Y.; Huang, B.J.; Hsu, Y.-T.; Khung, Y.L. Anti-Adhesion Behavior from Ring-Strain Amine Cyclic Monolayers Grafted on Silicon (111) Surfaces. *Sci. Rep.* **2020**, *10*, 8758. [[CrossRef](#)] [[PubMed](#)]
49. Mathioudaki, S.; Vandenabeele, C.R.; Tonneau, R.; Pflug, A.; Tennyson, J.; Lucas, S. Plasma polymerization of cyclopropylamine in a low-pressure cylindrical magnetron reactor: A PIC-MC study of the roles of ions and radicals. *J. Vac. Sci. Technol. A* **2020**, *38*, 033003. [[CrossRef](#)]
50. Wang, Y.H.; Moitreyee, M.R.; Kumar, R.; Shen, L.; Zeng, K.Y.; Chai, J.W.; Pan, J.S. A comparative study of low dielectric constant barrier layer, etch stop and hardmask films of hydrogenated amorphous Si-(C, O, N). *Thin Solid Film.* **2004**, *460*, 211–216. [[CrossRef](#)]
51. Laminack, W.; Gole, J.L.; White, M.G.; Ozdemir, S.; Ogden, A.G.; Martin, H.J.; Fang, Z.; Wang, T.-H.; Dixon, D.A. Synthesis of nanoscale silicon oxide oxidation state distributions: The transformation from hydrophilicity to hydrophobicity. *Chem. Phys. Lett.* **2016**, *653*, 137–143. [[CrossRef](#)]
52. Luo, L.; Song, Y.; Zhu, C.; Fu, S.; Shi, Q.; Sun, Y.-M.; Jia, B.; Du, D.; Xu, Z.-L.; Lin, Y. Fluorescent silicon nanoparticles-based ratiometric fluorescence immunoassay for sensitive detection of ethyl carbamate in red wine. *Sens. Actuators B Chem.* **2018**, *255*, 2742–2749. [[CrossRef](#)]
53. Eickhoff, T.; Medicherla, V.; Drube, W. Final state contribution to the Si 2p binding energy shift in SiO₂/Si(100). *J. Electron. Spectrosc. Relat. Phenom.* **2004**, *137–140*, 85–88. [[CrossRef](#)]
54. Seal, S.; Barr, T.L.; Krezoski, S.; Petering, D. Surface modification of silicon and silica in biological environment: An X-ray photoelectron spectroscopy study. *Appl. Surf. Sci.* **2001**, *173*, 339–351. [[CrossRef](#)]
55. Yoon, S.J.; Ryu, J.-H.; Ismail, M.; Chen, Y.-C.; Chang, Y.-F.; Yun, M.J.; Kim, H.-D.; Kim, S. Compliance current and temperature effects on non-volatile memory switching and volatile switching dynamics in a Cu/SiO_x/p++-Si device. *Appl. Phys. Lett.* **2019**, *115*, 212102. [[CrossRef](#)]
56. Biniak, S.; Szymański, G.; Siedlewski, J.; Świątkowski, A. The characterization of activated carbons with oxygen and nitrogen surface groups. *Carbon* **1997**, *35*, 1799–1810. [[CrossRef](#)]
57. Kubala-Kukuś, A.; Banaś, D.; Stabrawa, I.; Szary, K.; Sobota, D.; Majewska, U.; Wudarczyk-Moćko, J.; Braziewicz, J.; Pajek, M. Analysis of Ti and TiO₂ nanolayers by total reflection X-ray photoelectron spectroscopy. *Spectrochim. Acta Part B At. Spectrosc.* **2018**, *145*, 43–50. [[CrossRef](#)]
58. Ganguly, A.; Sharma, S.; Papakonstantinou, P.; Hamilton, J. Probing the Thermal Deoxygenation of Graphene Oxide Using High-Resolution In Situ X-ray-Based Spectroscopies. *J. Phys. Chem. C* **2011**, *115*, 17009–17019. [[CrossRef](#)]
59. Smith, M.; Scudiero, L.; Espinal, J.; McEwen, J.-S.; Garcia-Perez, M. Improving the deconvolution and interpretation of XPS spectra from chars by ab initio calculations. *Carbon* **2016**, *110*, 155–171. [[CrossRef](#)]
60. Effenberger, F.; Götz, G.; Bidlingmaier, B.; Wezstein, M. Photoactivated preparation and patterning of self-assembled monolayers with 1-alkenes and aldehydes on silicon hydride surfaces. *Angew. Chem. Int. Ed.* **1998**, *37*, 2462–2464. [[CrossRef](#)]
61. Indrawirawan, S.; Sun, H.; Duan, X.; Wang, S. Low temperature combustion synthesis of nitrogen-doped graphene for metal-free catalytic oxidation. *J. Mater. Chem. A* **2015**, *3*, 3432–3440. [[CrossRef](#)]
62. Bai, X.; Zhang, X.; Gu, H.; Li, F.; Huang, W.; Liang, L.; Ye, Z. Highly selective colorimetric sensing of Cu²⁺ using a Schiff base derivative immobilized on polyvinyl alcohol microspheres. *New J. Chem.* **2018**, *42*, 11682–11688. [[CrossRef](#)]
63. Kumar, B.; Asadi, M.; Pisasale, D.; Sinha-Ray, S.; Rosen, B.A.; Haasch, R.; Abiade, J.; Yarin, A.L.; Salehi-Khojin, A. Renewable and metal-free carbon nanofibre catalysts for carbon dioxide reduction. *Nat. Commun.* **2013**, *4*, 2819. [[CrossRef](#)]
64. Yan, Y.; Lin, J.; Jiang, J.; Wang, H.; Qi, J.; Zhong, Z.; Cao, J.; Fei, W.; Feng, J. A general strategy to construct N-doped carbon-confined MoO₂ and MnO for high-performance hybrid supercapacitors. *Vacuum* **2019**, *165*, 179–185. [[CrossRef](#)]
65. Vallée, A.; Humblot, V.; Méthivier, C.; Pradier, C.M. Glutathione adsorption from UHV to the liquid phase at various pH on gold and subsequent modification of protein interaction. *Surf. Interface Anal.* **2008**, *40*, 395–399. [[CrossRef](#)]

66. Gu, S.; Hsieh, C.-T.; Lin, T.-W.; Yuan, C.-Y.; Ashraf Gandomi, Y.; Chang, J.-K.; Li, J. Atomic layer oxidation on graphene sheets for tuning their oxidation levels, electrical conductivities, and band gaps. *Nanoscale* **2018**, *10*, 15521–15528. [[CrossRef](#)]
67. Wang, X.; Hu, Y.; Song, L.; Xing, W.; Lu, H.; Lv, P.; Jie, G. Flame retardancy and thermal degradation mechanism of epoxy resin composites based on a DOPO substituted organophosphorus oligomer. *Polymer* **2010**, *51*, 2435–2445. [[CrossRef](#)]
68. Wang, Y.Y.; Kusumoto, K.; Li, C.J. XPS Analysis of SiC Films Prepared by Radio Frequency Plasma Sputtering. *Phys. Procedia* **2012**, *32*, 95–102. [[CrossRef](#)]
69. Zou, J.; Dai, Y.; Pan, K.; Jiang, B.; Tian, C.; Tian, G.; Zhou, W.; Wang, L.; Wang, X.; Fu, H. Recovery of silicon from sewage sludge for production of high-purity nano-SiO₂. *Chemosphere* **2013**, *90*, 2332–2339. [[CrossRef](#)] [[PubMed](#)]
70. Khung, Y.L.; Ngalim, S.H.; Scaccabarozzi, A.; Narducci, D. Formation of stable Si-O-C submonolayers on hydrogen-terminated silicon(111) under low-temperature conditions. *Beilstein J. Nanotechnol.* **2015**, *6*, 19–26. [[CrossRef](#)] [[PubMed](#)]
71. Lehner, A.; Steinhoff, G.; Brandt, M.S.; Eickhoff, M.; Stutzmann, M. Hydrosilylation of crystalline silicon (111) and hydrogenated amorphous silicon surfaces: A comparative x-ray photoelectron spectroscopy study. *J. Appl. Phys.* **2003**, *94*, 2289–2294. [[CrossRef](#)]
72. López, G.P.; Castner, D.G.; Ratner, B.D. XPS O 1s binding energies for polymers containing hydroxyl, ether, ketone and ester groups. *Surf. Interface Anal.* **1991**, *17*, 267–272. [[CrossRef](#)]
73. Kim, Y.K.; Lee, H.S.; Yeom, H.W.; Ryoo, D.-Y.; Huh, S.-B.; Lee, J.-G. Nitrogen bonding structure in ultrathin silicon oxynitride films on Si(100) prepared by plasma nitridation. *Phys. Rev. B* **2004**, *70*, 165320. [[CrossRef](#)]
74. Chang, J.P.; Green, M.L.; Donnelly, V.M.; Opila, R.L.; Eng, J., Jr.; Sapjeta, J.; Silverman, P.J.; Weir, B.; Lu, H.C.; Gustafsson, T.; et al. Profiling nitrogen in ultrathin silicon oxynitrides with angle-resolved x-ray photoelectron spectroscopy. *J. Appl. Phys.* **2000**, *87*, 4449–4455. [[CrossRef](#)]
75. Ando, T.; Sumi, S.; Kawate, T.; Ichihara, J.; Hanafusa, T. Sonochemical switching of reaction pathways in solid-liquid two-phase reactions. *J. Chem. Soc. Chem. Commun.* **1984**, 439–440. [[CrossRef](#)]
76. Luche, J.L.; Einhorn, C.; Einhorn, J.; Sinisterra-Gago, J.V. Organic sonochemistry: A new interpretation and its consequences. *Tetrahedron Lett.* **1990**, *31*, 4125–4128. [[CrossRef](#)]
77. Kegelaers, Y.; Eulaerts, O.; Reisse, J.; Segebarth, N. On the quantitative measure of a sonochemical effect in heterogeneous sonochemistry. *Eur. J. Org. Chem.* **2001**, *2001*, 3683–3688. [[CrossRef](#)]
78. Martina, K.; Calsolaro, F.; Zuliani, A.; Berlier, G.; Chávez-Rivas, F.; Moran, M.J.; Luque, R.; Cravotto, G. Sonochemically-Promoted Preparation of Silica-Anchored Cyclodextrin Derivatives for Efficient Copper Catalysis. *Molecules* **2019**, *24*, 2490. [[CrossRef](#)]
79. Dickens, M.J.; Luche, J.-L. Further evidence for the effect of ultrasonic waves on electron transfer processes—the case of the Kornblum-Russell reaction. *Tetrahedron Lett.* **1991**, *32*, 4709–4712. [[CrossRef](#)]
80. Anto, T.; Bauchat, P.; Foucaud, A.; Fujita, M.; Kimura, T.; Sohmiya, H. Sonochemical switching from ionic to radical pathways in the reactions of styrene and trans- β -Methylstyrene with lead tetraacetate. *Tetrahedron Lett.* **1991**, *32*, 6379–6382. [[CrossRef](#)]
81. Ando, T.; Kimura, T.; Levêque, J.-M.; Lorimer, J.P.; Luche, J.-L.; Mason, T.J. Sonochemical Reactions of Lead Tetracarboxylates with Styrene. *J. Org. Chem.* **1998**, *63*, 9561–9564. [[CrossRef](#)]
82. Hickenboth, C.R.; Moore, J.S.; White, S.R.; Sottos, N.R.; Baudry, J.; Wilson, S.R. Biasing reaction pathways with mechanical force. *Nature* **2007**, *446*, 423–427. [[CrossRef](#)]
83. Cravotto, G.; Cintas, P. Power ultrasound in organic synthesis: Moving cavitation chemistry from academia to innovative and large-scale applications. *Chem. Soc. Rev.* **2006**, *35*, 180–196. [[CrossRef](#)] [[PubMed](#)]
84. Vinatoru, M.; Mason, T.J. Jean-Louis Luche and the interpretation of sonochemical reaction mechanisms. *Molecules* **2021**, *26*, 755. [[CrossRef](#)] [[PubMed](#)]
85. Paulusse, J.M.; Sijbesma, R.P. Reversible mechanochemistry of a PdII coordination polymer. *Angew. Chem. Int. Ed.* **2004**, *43*, 4460–4462. [[CrossRef](#)] [[PubMed](#)]
86. Yu, Y.; Hessel, C.M.; Bogart, T.D.; Panthani, M.G.; Rasch, M.R.; Korgel, B.A. Room temperature hydrosilylation of silicon nanocrystals with bifunctional terminal alkenes. *Langmuir* **2013**, *29*, 1533–1540. [[CrossRef](#)] [[PubMed](#)]
87. Andrews, D.R. Ultrasonics and Acoustics. In *Encyclopedia of Physical Science and Technology*, 3rd ed.; Meyers, R.A., Ed.; Academic Press: New York, NY, USA, 2003; pp. 269–287.